Supporting Information

Strong optical emission regulated by exciton state in two-dimensional organic molecular crystals

Yutian Yang[1], Ting Zheng[2], Weiwei Zhao[1]*, Chenyun Cao[1], Fang Yang[1]*, Hongwei Liu[1]*, Zhenhua Ni[2,3], Junpeng Lu[2,3]

[1] *Key Laboratory of State Manipulation and Advanced Materials in Provincial Universities, School of Physics and technology, Nanjing normal University, Nanjing 210023, China.*

[2]*Key Laboratory of Quantum Materials and Devices of Ministry of Education, School of Physics, Southeast University, Nanjing 211189, China.*

[3]*School of Electronic Science and Engineering, Southeast University, Nanjing, 210096, China*

*Corresponding author: Weiwei Zhao (jianpiao1986@163.com), Fang Yang (phyyf@nnu.edu.cn), Hongwei Liu (phylhw@njnu.edu.cn);

Supplementary Note 1: The fabrication of 2D organic molecular crystals

First, the Si/SiO_2 substrate were treated with oxygen plasma for 30s at 50 W in order to renders the substrate distinctly hydrophilic. Then, the pure C_8-BTBT powder were heated to 110°C in the center of a tube furnace, and the substrate with mechanically exfoliated few-layer h-BN were placed 10-12 cm away from it (in main text Figure 1a). Finally, heating the furnace to 110°C for 5 min under ultra-high vacuum condition (below 10^{-6} torr), ordered C_8-BTBT molecular crystal are formed through van der Waals epitaxial. At the distance of ~10-11 cm from the furnace center ($T \geq 100°C$), the h-BN substrate was completely covered by WL C_8-BTBT crystal in less than 5 min. Similarly, at the distance of ~11-12 cm from the center ($97°C < T < 100°C$), the graphene substrate was completely covered by multilayer C_8-BTBT crystal (1L-3L). When the distance from the center of the furnace was greater than 12 cm ($T < 97°C$), multiple layers C_8-BTBT crystal (3L to bulk) gradually accumulating as the growth

continued. The number of layers can be controlled by the heating temperature, growth duration and substrate position.

The oxygen plasma treatment renders the substrate distinctly hydrophilic, while the long C–H chains and benzene rings in the C_8-BTBT molecule are hydrophobic. Consequently, the adsorption energy between the organic molecules and the treated substrate is significantly reduced. As shown in Figure S2 (a), the thickness of the organic film grown on the untreated substrate is shown. The fitting results indicate that the thickness of the WL layer is 0.60 nm, the single layer (1L) is 2.34 nm, the double layer (2L) is 5.27 nm, and the triple layer (3L) is 8.12 nm. Figure S2(b) shows the thickness of the organic film grown on the substrate after oxygen plasma treatment. The thickness distribution is significantly larger than that on the untreated substrate. The fitted peaks are located at 0.82 nm (WL), 3.74 nm (1L), 6.67 nm (2L), and 9.52 nm (3L). This comparison result indicates that treating the substrate with O_2 plasma will make the thickness of the organic molecular layer thicker, suggesting that the oxygen plasma treatment has changed the adsorption behavior of organic molecules on the substrate.

The oxygen plasma treatment of the substrate causes most of the organic molecules to grow on the surface of h-BN, thereby significantly reducing the formation of thick molecular layers on the Si/SiO_2 substrate. This effectively reduces the interference from foreign molecules on the substrate in the experimental signal. At the same time, the formation of 1L molecules form a vertical structure like the thick layer, and no longer form a semi-inclined mode between WL and the thick layer. It provides a more ideal platform for us to directly study the transformation of H- and J-aggregation of organic molecular.

Supplementary Note 2: The aggregation of organic molecular crystals

As in our earlier works, we calculated the transition dipole moment (TDM) in WL and 1L C_8-BTBT crystal.[1] We have simplified the molecular arrangement scheme in WL C_8-BTBT crystal, the transition dipoles in the molecule are arranged parallel within

the basal plane. The arrangement structure of WL C_8-BTBT crystal is shown in Figure 1 (b) of the main text. From the axial perspective of the transition dipole, both the nearest neighbor and the second nearest neighbor molecules are both in parallel directions. In Kasha's model, the geometries that lead to J- and H-aggregates are predicated on long-range Coulomb coupling alone.[2, 3] The Coulomb coupling (J_{Coul}) between any two chromophores arises from the interaction between their transition charge distributions and is often expressed using the point-dipole approximation,[4]

$$J_{Coul} \approx \frac{\mu^2(cos\alpha - 3\cos\theta_1\cos\theta_2)}{4\pi\varepsilon R^3} \quad (1)$$

where R is the intermolecular distance between mass centers, μ is the transition dipole moment, θ_1 and θ_2 are the angles between μ and R, and ε is the optical dielectric constant of the medium. Considering the angles of the nearest and second-nearest neighbor molecules in WL and substituting them into the above eq.(1) for calculation. The nearest-neighbor coupling in WL C_8-BTBT organic crystals is positive ($J_{Coul} > 0$) and the next-nearest-neighbor coupling is negative ($J_{Coul} < 0$) [5]. The nearest-neighbor coupling in 1L C_8-BTBT organic crystals is negative ($J_{Coul} < 0$), which enabled to form J-aggregates through intra-chain Coulombic interactions.

Supplementary Note 3: The aggregated Hamiltonian and excited state in molecular crystal

In order to describe the properties of excitons in aggregated molecular crystal, we utilize the Hamiltonian, H, describe as below[6],

$$H = \omega \sum_n b_n^* b_n + \omega\lambda \sum_n (b_n^* + b_n)|n\rangle\langle n| + \sum_m \sum_n J_{mn}|m\rangle\langle n| + (\lambda^2 + 1)\omega \quad (2)$$

where $b_n^* b_n$ are creation and annihilation operators corresponding to the symmetric intramolecular vibrational mode on molecule n, and $\mathbf{n}\rangle$ is the pure electronic state in which the molecule is excited to the excited state while others remain electronically unexcited. Assuming periodic boundary conditions and treating H using a single molecule per unit cell leads to aggregate excited states or excitonic polarons with wave vector k. The first Brillouin zone of the simplified square M×M aggregates consist of the wave vectors,

$$k = k_1(d_1/d^2) + k_2(d_2/d^2) \quad (3)$$

where, $d \equiv |d_1| = |d_2|$ and where the allowed values of the dimensionless wave vector index, k_i, are given by, $k_i = 0, \pm 2\pi/M, \ldots, \pi$ (taking M even) for an M×M aggregate with a total of $N = M^2$ molecules. In the free exciton limit, using eq.(3), leads to H-like aggregates with a weakly allowed b-polarized lower band edge having $k = (\pi, \pi)$ and a strongly allowed ac-polarized upper band edge having $k = (0, 0)$, corresponding to the lower and upper Davydov components, respectively. In particular, the lower Davydov exciton exhibits a sign change between the two molecules in the unit cell (as does the $k = (\pi, \pi)$ exciton in the notation of this work), unlike the upper Davydov exciton.

Supplementary Note 4: Experimental method of Raman and PL spectroscopy

Raman spectroscopy was performed by Witec400 spectrometer coupled to a silicon CCD camera (Princeton Instruments PYL-1300BXD). We use a 355 nm laser as excitation source, and Raman signal was collected by a 40× ultraviolet object lens. The PL spectra were obtained with a laser confocal microscope (THORLABS Spectra) in back scattering geometry with 325 nm excitation lasers and the power was kept below 0.1mW to avoid laser-induced heating. The signal was collected with a 40× ultraviolet object lens with NA = 0.5 and the laser spot size was about 1 μm in diameter.

Photo-oxidation and photobleaching can be effectively avoided in a vacuum and low-temperature environment. To ensure the accuracy and reliability of PLQY data, we study the PLQY of organic materials in a vacuum system (below 10^{-1} pa) using a 355 nm laser with a power range of 0.1–40 μW. Additionally, we verify the stability of the emission intensity throughout the photoluminescence measurement and use sufficiently low excitation densities to minimize artifacts from heating and oxidation.

Supporting Information Figure S1

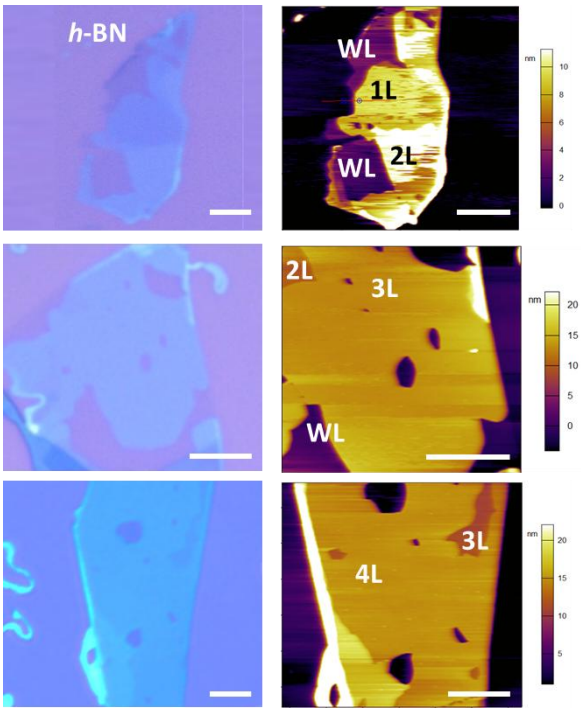

Figure S1 Characterization of C_8-BTBT molecular crystal on *h*-BN. The optical microscope (left) and AFM images (right) of PVD growth C_8-BTBT molecular crystal on *h*-BN. The scale bar is 10 μm.

Supporting Information Figure S2

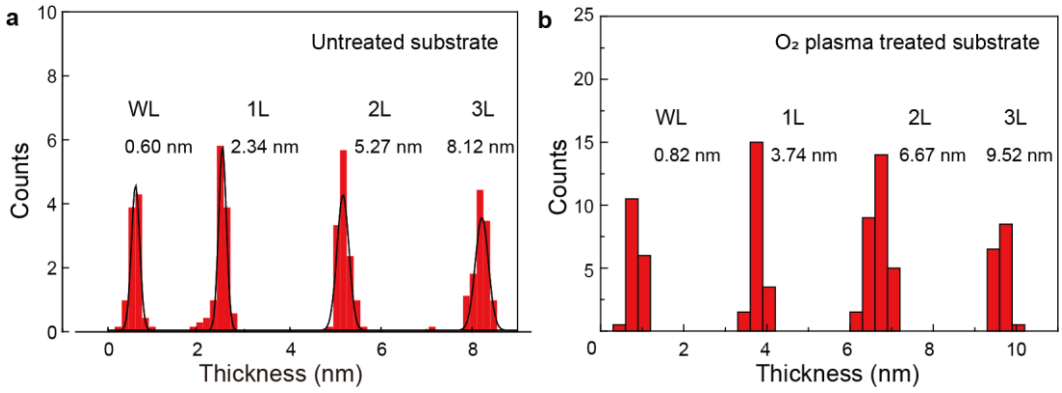

Figure S2 The statistical distribution of layer thickness distribution of C_8-BTBT molecular crystal grown on two different substrates, comparing (a) an untreated substrate and (b) an O_2 plasma-treated substrate.

Supporting Information Figure S3

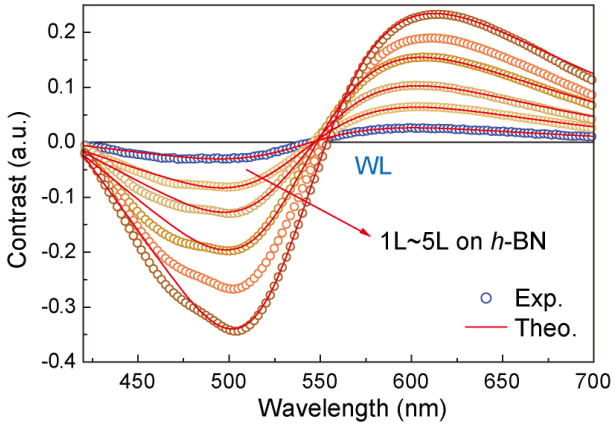

Figure S3 The optical contrast of C_8-BTBT molecular crystal on *h*-BN. The experimental (dots) and theoretically calculated (red line) optical contrast spectra (C'(λ)) of C_8-BTBT molecular crystal from WL to 5L.

Supporting Information Figure S4

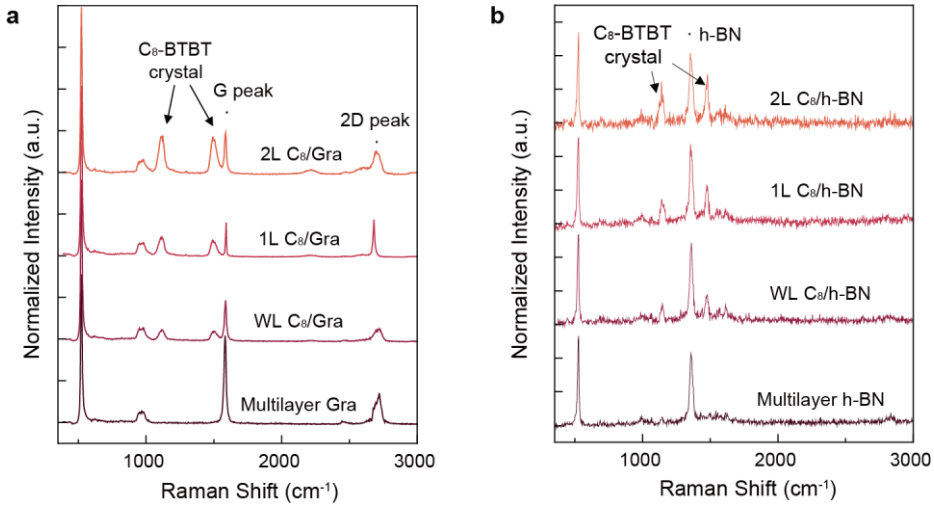

Figure S4. (a, b) Raman spectra of the C_8-BTBT molecule crystals with different layers (WL, 1L and 2L) on (a) graphene and (b) h-BN substrate.

Supporting Information Figure S5

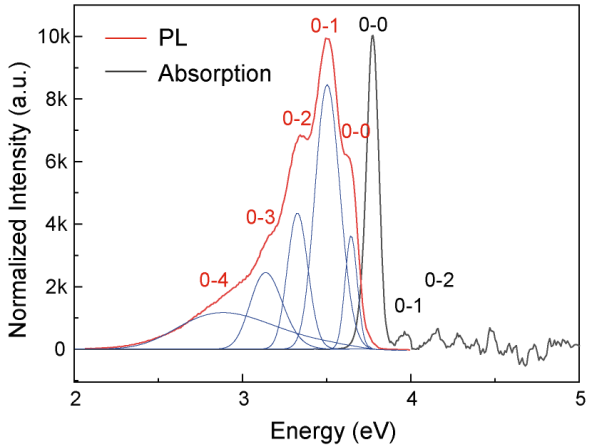

Figure S5 The absorption and PL spectra of C_8-BTBT molecules in solution. The excitation was made by the same 305 nm CW laser line and laser power of 50 μW.

Supporting Information Figure S6

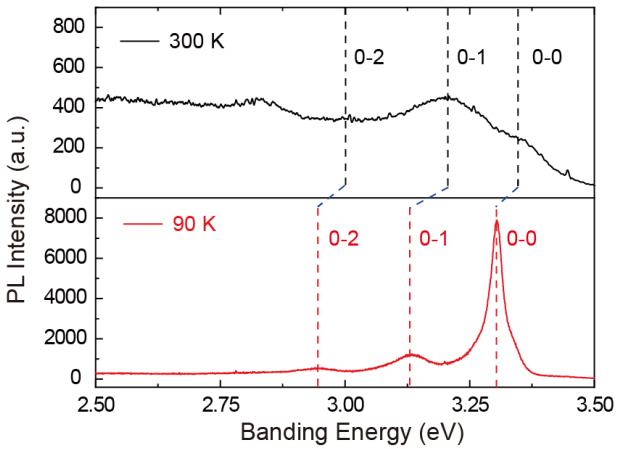

Figure S6 The PL spectra of WL C_8-BTBT crystals at room temperature and low temperature. Compared with the non-uniform energy levels between emission bands at room temperature, the energy intervals between the emission bands are all 0.18 eV at low temperatures.

Supporting Information Figure S7

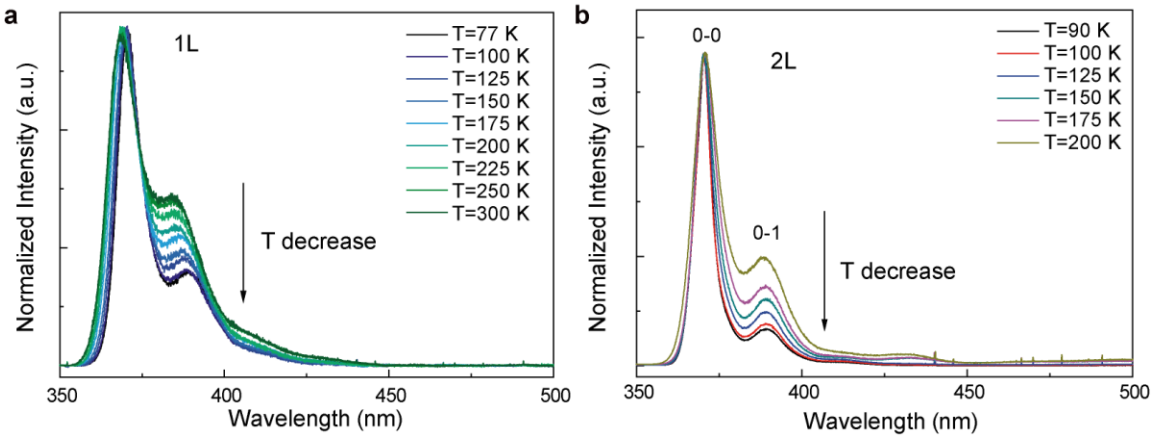

Figure S7 The temperature dependence PL spectra of (a) 1L and (b) 2L C_8-BTBT crystals. There is a redshift of the 0-0 band and 0-1 band in 1L, and the significant increase the R_{01} is a clear observed in both 1L and 2L. It can also be observed that the full width at half maxima (FWHM) of the 0-0 band narrates significantly as the temperature decreases, revealing a distinct superradiation phenomenon at low temperatures.

Supporting Information Figure S8

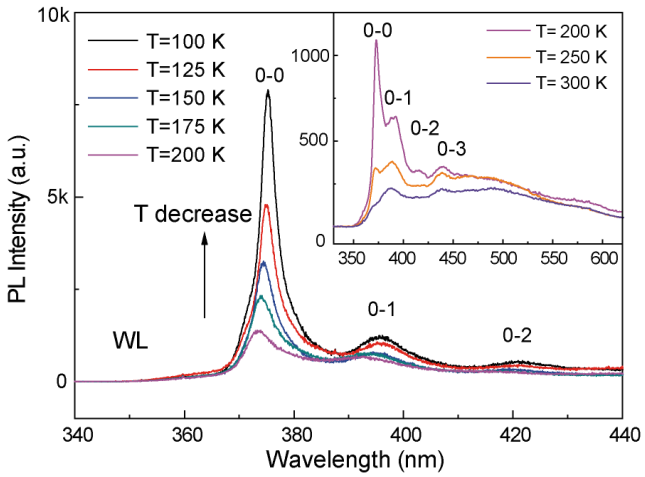

Figure S8 The temperature dependence PL spectra of WL C_8-BTBT crystals. The insert picture shows the PL intensity in the 0-0 band increases significantly at 200K, illustrated that the dark excitons in the 0-0 exciton band transform into bright excitons.

Supporting Information Figure S9

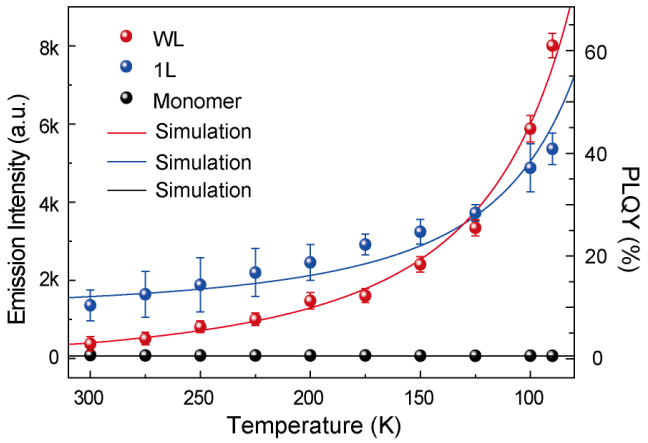

Figure S9 The temperature dependence of the 0-0 band emission intensity and simulation for WL, 1L, and monomer samples. There is a deviation between the simulated and experimental data is observed for the 1L J-aggregate film around 150 K. It is attribute to the higher density of structural defects in the J-aggregate crystals. As the layer number increases, it is likely introducing more defects in 1L. These defects dominate exciton localization around 150 K, causing the deviation from the ideal thermal behavior.

Reference:

[1] Yang Y, Wang Y, Qiao J, et al. Aggregation-Dependent Dielectric Permittivity in 2D Molecular Crystals. Small Methods, 2022, 6: e2101198.

[2] Kasha M. Energy Transfer Mechanisms and the Molecular Exciton Model for Molecular Aggregates. Radiation Research, 2012, 178: AV27-AV34.

[3] Hochstrasser R M, Kasha M. APPLICATION OF THE EXCITON MODEL TO MONOMOLECULAR LAMELLAR SYSTEMS. Photochemistry and Photobiology, 1964, 3: 317-331.

[4] Hestand N J, Spano F C. Molecular Aggregate Photophysics beyond the Kasha Model: Novel Design Principles for Organic Materials. Accounts of Chemical Research, 2017, 50: 341-350.

[5] Yang Y, Wang Y, Qiao J, et al. Aggregation-Dependent Dielectric Permittivity in 2D Molecular Crystals. Small Methods, 2022, 6: 2101198.

[6] Spano F C. Temperature-dependent emission in disordered herringbone aggregates of conjugated oligomers. Physical Review B, 2005, 71: 235208-235213.